# Palm Vein Recognition Based on 2D Gabor Filter and Artificial Neural Network

Rabikumar Meitram and Prakash Choudhary
Computer Science and Engineering Department, National Institute of Technology Manipur, Imphal, 795001, India
Email: {rabimeitramcha, choudharyprakash87}@gmail.com, choudharyprakash@nitmanipur.ac.in

***Abstract*—This paper presents a new approach to improve the performance of palm vein-based identification systems. Here palm vein is considered as a piece of texture and apply texture-based feature extraction technique. The palm vein from the database is used to identify the Region of Interest of that particular palm vein image. The extracted Region of Interest is than applied Gabor Filter for local features extraction. Extracted local features are then applied sequential feature reduction to reduce the features which are more unique. Reduced features vectors are then process using artificial neural network environment.**

***Index Terms*—palm vein, Gabor filter, ANN, Gaussian filter, ROI**

## I. Introduction

Biometrics is the automated methods of recognizing a person based on a physiological or behavioral characteristic. Among the features measured are the face, fingerprint, hand geometry, iris, retinal, signature, gait, voice, palm vein etc. Biometric technologies are becoming the foundation of an extensive array of highly secure identification and personal verification solutions. As the level of security breaches and transaction fraud increases, the need for highly secure identification and personal verification technologies is becoming apparent.

Biometric-based solutions are able to provide for confidential financial transactions and personal data privacy. The need for biometrics can be found in central government, state and local governments, in the military, and in commercial applications. Enterprise-wide network security infrastructures, government IDs, secure electronic banking, investing and other financial transactions, retail sales, law enforcement, and health and social services are already benefiting from these technologies.

Biometric-based authentication applications include workstation, network, and domain access, single sign-on, application logon, data protection, remote access to resources, transaction security and Web security. Trust in these electronic transactions is essential to the healthy growth of the global economy. Utilized alone or integrated with other technologies such as smart cards, encryption keys and digital signatures, biometrics is set to pervade nearly all aspects of the economy and our daily lives. Utilizing biometrics for personal authentication is becoming convenient and considerably more accurate than current methods (such as the utilization of passwords or PINs). This is because biometrics links the event to a particular individual (a password or token may be used by someone other than the authorized user), is convenient (nothing to carry or remember), accurate (it provides for positive authentication), can provide an audit trail and is becoming socially acceptable and inexpensive [1].

Broadly, biometric identification characteristics are classified into two broad categories: behavioral and physiological characteristics Fig. 1.

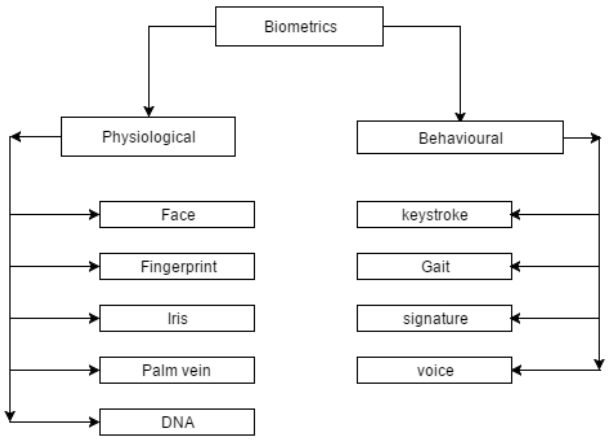


Figure 1. Classification of biometrics.

Behavioral biometrics is the field of study related to the measurement of uniquely identifiable and measurable patterns in human activities such as keystroke, signature, voice etc. Whereas, the physical biometrics involves in the measurement of the innate human characteristics such as fingerprints, face, iris patterns, palm vein etc.

Palm vein authentication has a high level of authentication accuracy due to the uniqueness and complexity of vein patterns of the palm. The palm vein patterns are internal to the body; thus, it is very difficult to forge. Also, the system is contactless and hygienic for use in public areas. Vein patterns are unique to each individual; even identical twins have different vein patterns. It is more powerful than others biometric authentication such as face, iris, and retinal [2].

For sample collection, palm has wide area and more complicated vascular pattern and contains some differentiation for personal identification when compare with the patterns present in the back of the hand and

Manuscript received January 20, 2018; revised July 20, 2018.

© 2018 J. Adv. Inf. Technol.
doi: 10.12720/jait.9.3.68-72

ventral or dorsal side of the fingers. The palm normally has no hair and thus eliminates and obstacles to capturing the vein pattern and it is less susceptible to a change in skin color.

A contactless palm vein authentication device was launched by Fitjutsu in Japan under the name 'palmsecure'. Table I shows the results of various biometrics techniques according to Fijitsu. False Acceptance Rate (FAR) of less than 0.00008% for palm vein are based on the experiments conducted on 70,000 individuals in Japan by Fijutsu Company.

TABLE I. COMPARISON OF DIFFERENT BIOMETRIC MODALITIES*

| Technology | FAR (%) | FRR (%) |
|---|---|---|
| Voice Recognition | 2.00 | 10.00 |
| Fingerprint | 1--2 | 3.00 |
| Iris | .0001--0.94 | –0.99--0.2 |
| PalmSecure | 0.00008 | 0.01 |

*FAR, false acceptance rate; FRR, false rejection rate.

Palm vein biometrics is taken as the area for the project as it is one of the most secure biometric measurements among the different biometrics measures. And also, palm vein biometrics provides a great scope for its applications in financial institutions and on personal authentication system.

## II. FINDING THE REGION OF INTEREST (ROI)

Image segmentation is one of the most important steps in the analysis of processed image data. Its main goal is to separate components of the object image that have a strong relevance to the analysis from the background. When a palm image is obtained, the palm background is first segmented from the image [3]. Binarization is used to segmenting the image into two levels; object (palm region) and background. For palm image segmentation, Otsu's thresholding is applied to the palm image to estimate the palm region. By comparing the segmented palm shapes with the original palm images, we can see that they are almost indistinguishable as shown in Fig. 2(a) and (b). This shows that Otsu's method is quite effective in determining the threshold of palm images.

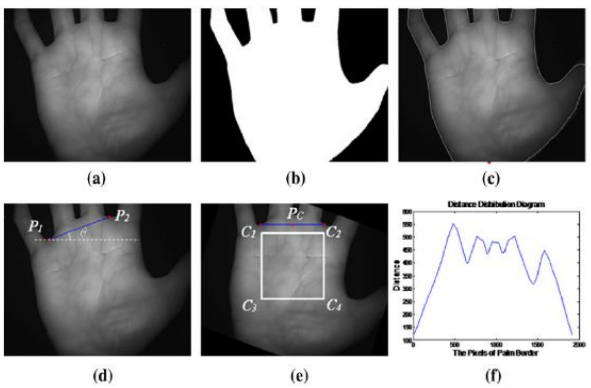


Figure 2. Finding the ROI of the input palm vein image, (a) the original palm vein image, (b) the palm vein is segmented using Otsu's method, (c) the palm border is extracted by inner border tracing algorithm, (d) two datum points P1 and P2 are selected, and rotated and angle to make it parallel to horizontal axis, (e) the region C1C2C3C4 is the required ROI, (f) the distance distribution diagram of palm border.

To increase verification accuracy and reliability, the features of vein patterns extracted from the same region in different palm vein images are compared for verification. The region to be extracted is known as the ROI. For this reason, it is important to fix the ROI in the same position in different palm vein images to ensure the stability of the principal extracted vein features. However, it is difficult to fix the ROI at the same position in different palm vein images without the use of a docking device to constrain the palm position when acquiring palm vein images.

In this paper, we have employed the two data points, $P_1$ and $P_2$ as shown in Fig. 2(d), to determine the approximate (not absolute) immovable ROI [4]. The following processes are performed to determine the two data points in binary palm vein images. First, the inner border tracing algorithm is employed to find the palm border [5]. Fig. 2(e) shows an example of illustrating how the extracted border of a palm image which perfectly matches the original palm contours. Then for each point on the palm contour, the distance between this point and the mid-point of the wrist is calculated. Fig. 2(f) shows the distance distribution diagram. As seen, there are five local maximums and four local minimums. The pattern in the diagram is quite similar to the geometric shape of a palm (Fig. 2(a)), which also has five tips (local maximums) and four finger-webs (local minimums). Experimenting on a wide variety of palm vein images, we found that the four local minimum locations in the distance distribution diagram are the same as finger-web locations and match between the two locations is very close. Finally, two valley points, $P_1$ (the valley point between the small finger and ring finger) and $P_2$ (the valley point between the middle finger and the index finger), are selected as two key data points, as shown in Fig. 2(d). These two data points ($P_1$ and $P_2$) are employed to locate the ROI. The procedure is described as follows.

- First, the straight line $P_1P_2$ is formed by the points of $P_1$ and $P_2$ as shown in Fig. 2(d). To eliminate the influences of palm rotation and define the coordinates of ROI more conveniently, the palm image is rotated by the angle, h between line $P_1P_2$ and the horizontal (1).

$$\Theta = tan^{-1}(Y_{P_2} - Y_{P_1})/(X_{P_2} - X_{P_1}) \quad (1)$$

where, $(X_{P_1}, Y_{P_1})$ is the coordinate of $P_1$ and $(X_{P_2}, Y_{P_2})$ is the coordinate of $P_2$.

This makes the direction of line $P_1P_2$ is horizontal, as shown in Fig. 2(e). A rectangular region $C_1C_2C_3C_4$ whose corners are $C_1$, $C_2$, $C_3$ and $C_4$ is located and denoted as the ROI. The length of line $C_1C_2$ and line $P_1P_2$ are equal. The Line $C_1C_2$ and $C_2C_4$ are vertical.

Finally, we redefine the original co-ordinate (0,0) at the upper-left point $C_1$ of the ROI. The reason for extracting the ROI in this manner is that, this ensures all the ROIs reference the same region in the palm vein image. In this way, we can overcome the problem of not using docking devices while acquiring palm vein images. High verification accuracy can simultaneously be maintained.

© 2018 J. Adv. Inf. Technol.

## III. ROI SKELETONIZATION

By observing the cross-sections of ROI, we found that they are Gaussian shape lines. Fig. 2(a) shows some cross-sections of the palm veins. Based on this observation, a multiscale matched filter scheme is used to detect palm vein and to improve the performance of vein detection. This scheme includes multiscale matched filters and scale production. The matched filter is define as

$$g_\phi = -\exp\left(-\frac{x'^2}{\sigma_x^2}\right) - m, \text{ for}$$

$$|x'| \le 3\sigma_x \rightarrow |y'| \le L/2 \quad (2)$$

$$x' = x\cos\phi + y\sin\phi$$
$$y' = y\cos\phi - x\sin\phi$$

where, $\phi$ is the filter direction, $\sigma$, standard deviation of Gaussian, $m$, the mean value of the filter, and $L$, is the length of the filter in y-direction which is set according to experience (2) [6]. This filter can be regarded as Gaussian filter in x-direction. A Gaussian shaped filter can help to denoise and the zero-sum can help to suppress the background pixels.

The filtered images are being used for extracting the feature vectors using 2D Gabor filters. (Fig. 3)

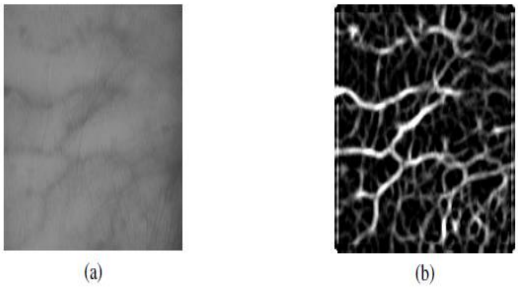


Figure 3. (a) Selected ROI of the input image, (b) single-scale matched filter response.

## IV. FEATURE EXTRACTION USING GABOR FILTER

Marcelja and Daugman modelled the responses of the visual cortex by Gabor functions because they are similar to the receptive field profiles in the mammalian cortical simple cells [7]-[9]. Gabor filters are extremely useful for texture analysis because of the 2D spectral specificity of texture as well as its variation with 2D spatial position. Daugman developed the 2D Gabor functions (a series of local spatial bandpass filters), which have good spatial localization, orientation selectivity, and frequency [8], [9]. A circular 2D Gabor filter is an oriented complex sinusoidal grating modulated by 2D Gaussian function, which is given by

$$G_{\sigma,\mu,\theta}(x,y) = g_\sigma(x,y).\exp[2\pi j\mu(x\cos\theta + y\cos\theta)] \quad (3)$$

where,

$$g_\sigma(x,y) = \left(1/2\pi\sigma^2\right).\exp[-\frac{x^2+y^2}{2\sigma^2}]$$

and $j = \sqrt{-1}$.

The frequency of the span-limited sinusoidal grating is given by $\mu$ and its orientation is specified as $\theta$; gσ(x,y), the Gaussian function and $\sigma$ is the standard deviation of the Gaussian envelope. The parameters of a 2D Gabor filter are therefore given by the frequency, μ, the orientation θ and the standard deviation σ. Note that we need only to consider θ in the interval [0°, 180°]. To analysis the 2D Gabor filter in terms of the real and imaginary parts, we express Eq. (3) in the complex form

$$G_{\sigma,\mu,\theta}(x,y) = R_{\sigma,\mu,\theta}(x,y) + jI_{\sigma,\mu,\theta}(x,y)$$

where, $R_{\sigma,\mu,\theta}(x,y) = g_\sigma(x,y)\cdot\cos[2\pi\mu(x\cos\theta + y\sin\theta)]$
$I_{\sigma,\mu,\theta}(x,y) = g_\sigma(x,y)\cdot\sin[2\pi\mu(x\cos\theta + y\sin\theta)]$

Such 2D Gabor filters are widely used as tunable filters for extracting the orientation or edge information from images. Lee gave a good introduction to image representation by using Gabor functions [10]. Daugman applied the 2D Gabor filter for iris recognition technology; because it can offer good distinguish ability in both frequency and space domains with very high speed. In most application, they are bandpass filters, which are inspired by a multi-channel filtering theory for processing visual information in the early stages of the human visual system [9], [11], [12]. The input image is generally filtered by a family of 2D Gabor filters tuned to several resolutions and orientations. However, it may not be computationally convenient or feasible to apply a large number of filters responding at multiple resolutions and orientations to an image.

Gabor filter consists of two parts (a) Gabor filter bank part and (b) Gabor features extraction part. Gabor filter banks parts generate a custom Gabor filter bank. It creates a u by v cell array, whose elements are m by n matrices; each matrix being a 2D Gabor filter, whereas Gabor features extraction parts extract the Gabor features of an input image. It creates a column vector, consisting of the Gabor features of the input image. The feature vectors are normalized to zero mean and unit variance (around 5000 approx.). (Fig. 4)

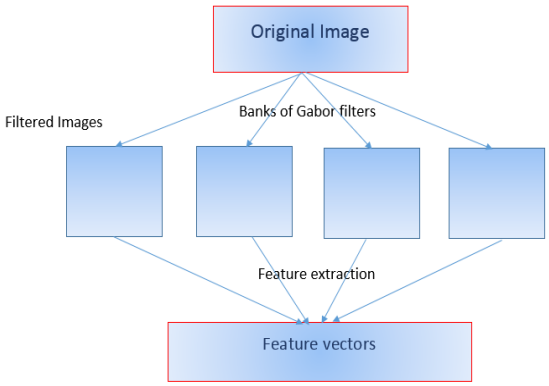


Figure 4. Gabor filter banks and extracted features.

## V. SEQUENTIAL FEATURE REDUCTION

As the number of features extracted by the Gabor filter is very large, we apply a sequential feature selection in order to reduce the feature vectors. Given below is the code to reduce the feature vectors. After reduction each images have only 34 feature vectors.

© 2018 J. Adv. Inf. Technol.

```
X = X + 0.01*rand(size(X));
[y,~] = find(target);
c = cvpartition(y,'k',50);
opts = statset('disp','iter');
fun = @(XT,yT,Xt,yt) (sum(yt ~=
classify(Xt,XT,yT,'linear')));
[fs,history] = sequentialfs(fun,X,y,'cv',c,'options',opts).
```

After extracting features vectors, the database is divided into two categories. First database is used to store the training feature vectors. And second for store testing feature vectors. Selection of testing database is in such a way that only one feature vector per person is there.

## VI. Classification and Training

The classification of the input feature vectors is done in an artificial neural network environment of Matlab. And training is done using two layers, and function used is Levenberg–Margquardt algorithm. After creating a network in Matlabnntool, training parameter is changed, for goal = 0.0001 and max fail = 100 and the rest remain the default parameters.

## VII. Experimental Results

The confusion matrix is plot between target and calculated output.

From Fig. 5, we can conclude that the output class are almost similar with similarity of 97.5% of the output confusion matrix.

From the performance validation graph as shown in Fig. 6, we can conclude that the performance of the training parameters increases with time.

Regression analysis graph between training, testing and validation parameters are all showing high degree of accuracy. So the performance and purposes for the biometric system is very high (Fig. 7).

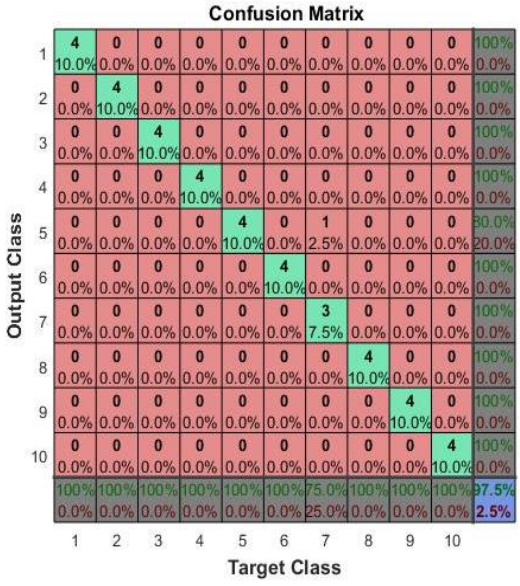


Figure 5. Confusion matrix.

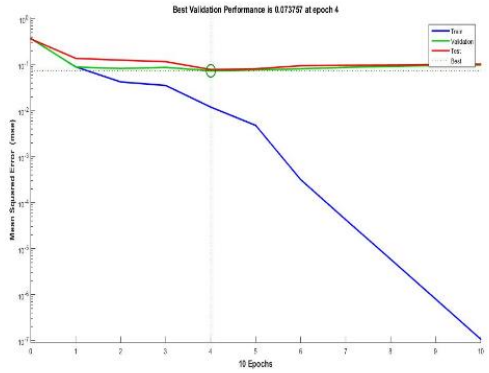


Figure 6. Validation performance.

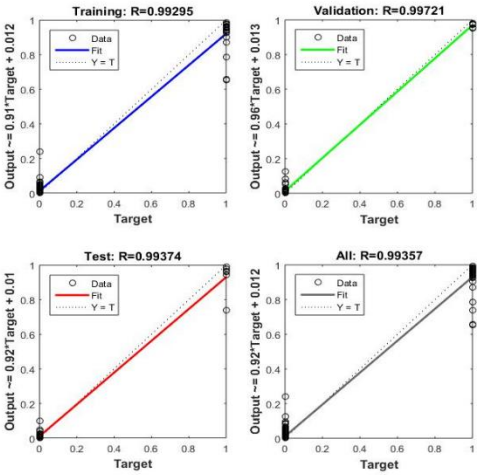


Figure 7. Regression graph.

We have tested the proposed biometric identification system using palm vein images of 100 persons. And out of the 100 persons 92 persons can be identified correctly by this system [13].

## VIII. Conclusion

The propose technique resulted with high efficiency and accuracy according to the above confusion matrix, performance validation, regression graphs etc. so this techniques is can be used of palm vein authentication.

## References

[1] R. C. Rahul, M. Cherian, and C. M. M. Mohan, "Literature survey on contactless palm vein recognition," *International Journal of Computer Science Trends and Technology*, vol. 3, pp. 1–6, 2015.

[2] W. Lingyu and G. Leedham, "Near- and far-infrared imaging for vein pattern biometrics," in *Proc. IEEE International Conference on Video and Signal Based Surveillance*, 2006.

[3] C. Haifen, L. Guangming, and W. Rui, "A new palm vein matching method based on ICP algorithm," in *Proc. 2nd International Conference on Interaction Sciences: Information Technology, Culture and Human*, Nov. 2009, pp. 1207–1211.

[4] M. Pan and W. Kang, "Palm vein recognition based on three local invariant feature extraction algorithms," in *Biometric Recognition*, Z. Sun, *et al*., Eds., Berlin Heidelberg: Springer-Verlag, 2011, pp. 116–124.

[5] M. Sonka, V. Hlavoc, and R. Boyle, *Image Processing Analysis and Machine Vision*, 2nd ed., Pacific Grove, CA: Brooks/Cole Publishing Company, 1999.

© 2018 J. Adv. Inf. Technol.

[6] Y. B. Zhang, Q. Li, J. You, and P. Bhattacharya, "Palm vein extraction and matching for personal authentication," in *Advances in Visual Information Systems*, G. Qiu, *et al.*, Eds., Springer Berlin Heidelberg, 2007.
[7] S. Marcelja, "Mathematical description of the responses of simple cortical cells," *Journal of the Optical Society of America*, vol. 70, pp. 1297–1300, 1980.
[8] J. G. Daugman, "Two-dimensional spectral analysis of cortical receptive field profiles," *Vision Research*, vol. 10, pp. 847–856, 1980.
[9] J. G. Daugman, "Uncertainty relation for resolution in space, spatial frequency, and orientation optimized by two-dimensional visual cortical filters," *Journal of the Optical Society of America*, pp. 1160–1169, 1985.
[10] J. C. Lee, C. H. Lee, C. B. Hsu, P. Y. Kuei, and K. C. Chang, "Dorsal hand vein recognition based on 2D Gabor filters," *The Imaging Science Journal*, vol. 62, 2014.
[11] J. G. Daugman, "High confidence visual recognition of persons by a test of statistical independence," *IEEE Transactions on Pattern Analysis and Machine Intelligence*, vol. 15, pp. 1148–1161, 1993.
[12] D. Gabor, "Theory of communication," *Journal of the Institution of Electrical Engineers*, vol. 93, pp. 429–441, 1946.
[13] W. Y. Han and J. C. Lee, "Palm vein recognition using adaptive Gabor filter," *Expert Systems with Applications*, vol. 39, pp. 13225–13234, 2012.

**Rabikumar Meitram** received his M.Tech degree from National Institute of Technology Manipur, India in 2016. His research area includes pattern recognition, feature extraction, artificial intelligence, deep learning, image annotation and retrieval, image processing, bio-medical image processing, and image classification.

**Prakash Choudhary** received his B.E. degree in Information Technology in 2009 from University of Rajasthan, Jaipur, India. He received M. Tech degree in Computer Science and Engineering from Visvesvaraya National Institute of Technology, Nagpur, India, in 2012, and Ph.D. degree from the Malaviya National Institute of Technology, Jaipur, India in 2016. He is working as an Assistant Professor in National Institute of Technology, Manipur, India from December 2013. His area of research interests are Image analysis, corpus development, computer vision and pattern recognition.

© 2018 J. Adv. Inf. Technol.